AUGUST 1994

ECN-RX--94-056

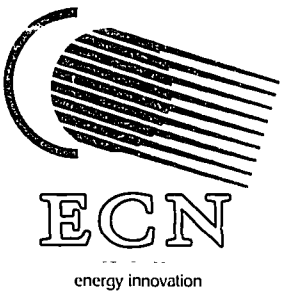

SAFETY CONSEQUENCES OF THE RELEASE OF RADIATION INDUCED STORED ENERGY

J. PRIJ

The Netherlands Energy Research Foundation ECN is the leading institute in the Netherlands for energy research. ECN carries out basic and applied research in the fields of nuclear energy, fossil fuels, renewable energy sources, policy studies, environmental aspects of energy supply and the development and application of new materials.

ECN employs more than 900 staff. Contracts are obtained from the government and from national and foreign organizations and industries.

ECN's research results are published in a number of report series, each series serving a different public, from contractors to the international scientific world.

This RX-series is used for publishing pre-prints or reprints of articles that will be or have been published in a journal, or in conference or symposium proceedings.

Please do not refer to this report but use the reference provided on the title page: 'Submitted for publication to ...' or 'Published in ...'.

Het Energieonderzoek Centrum Nederland (ECN) is het centrale instituut voor onderzoek op energiegebied in Nederland. ECN verricht fundamenteel en toegepast onderzoek op het gebied van kernenergie, fossiele-energiedragers, duurzame energie, beleidsstudies, milieuaspecten van de energievoorziening en de ontwikkeling en toepassing van nieuwe materialen.

Bij ECN zijn ruim 900 medewerkers werkzaam. De opdrachten worden verkregen van de overheid en van organisaties en industrieën uit binnen- en buitenland.

De resultaten van het ECN-onderzoek worden neergelegd in diverse rapportenseries, bestemd voor verschillende doelgroepen, van opdrachtgevers tot de internationale wetenschappelijke wereld.

Deze RX-serie wordt gebruikt voor het uitbrengen van pre-prints of reprints van artikelen die in een tijdschrift of in proceedings van conferenties of symposia (in definitieve vorm) zullen verschijnen of al zijn verschenen.

Gelieve niet te refereren aan het rapportnummer, maar de verwijzing te gebruiken die hiernaast op de titelpagina figureert: 'Voor publikatie aangeboden aan ...' of 'Verschenen in ...'.

Netherlands Energy Research Foundation ECN
P.O. Box 1
NL-1755 ZG Petten
the Netherlands
Telephone : +31 2246 49 49
Fax : +31 2246 44 80

This report is available on remittance of Dfl. 35 to:
ECN, General Services,
Petten, the Netherlands
Postbank account No. 3977703.
Please quote the report number.

Energieonderzoek Centrum Nederland
Postbus 1
1755 ZG Petten
Telefoon : (02246) 49 49
Fax : (02246) 44 80

Dit rapport is te verkrijgen door het overmaken van f 35,-- op girorekening 3977703 ten name van:
ECN, Algemene Diensten
te Petten
onder vermelding van het rapportnummer.

AUGUST 1994

ECN-RX--94-056

SAFETY CONSEQUENCES OF THE RELEASE OF RADIATION INDUCED STORED ENERGY

J. PRIJ

TO BE SUBMITTED TO: NUCLEAR TECHNOLOGY

ABSTRACT

Due to the disposal of high-level waste (HLW) in a salt formation gamma-energy will be deposited in the rock salt. Most of this energy will be converted into heat, whilst a small part will create defects in the salt crystals. It has been shown that energy is stored in the damaged crystals. Due to uncertainties in the models and differences in the disposal concepts the estimated values for the stored energy range from 10 to 1000 J/g in the most heavily damaged crystals close to the waste containers. The amount of radiation damage decays exponentially with increasing distance from the containers and at distances larger than 0.2 m the stored energy can be neglected. Given the uncertainties in the model predictions and in the possible release mechanism this report concludes that at this moment an instantaneous release of stored energy cannot be excluded completely. Therefore the thermo-mechanical consequences of a postulated instanteous release of an extremely high amount of radiation induced stored penergy have been estimated. These estimations are based on the quasi-static solutions for line and point sources. To account for the dynamic effects and the occurrence of fractures an amplification factor has been derived from mining experience with explosives. A validation of this amplification factor has been given using post experimental observations of two nuclear explosions in a salt formation. For some typical disposal concepts in rock salt the extent of the fractured zone has been estimated. It appeared that the radial extent of the fractured zone is limited to 5 m. Given the much larger distance between the individual boreholes and the distance between the boreholes and the boundary of the salt formation (more than 100 m), it is concluded that the probability of a release of radiation induced stored energy creating a pathway for the nuclides from the containers to the groundwater, is extremely low. The radiological consequences of a groundwater intrusion scenario induced by this very unprobable pathway are bounded by the 'standard' groundwater intrusion-extrusion scenario used in the performance assessment (smaller than 10^{-8} Sv/a).

CONTENT

1. INTRODUCTION

Due to the disposal of high level waste (HLW) in a salt formation gamma energy will be deposited in the rock salt. Most of this energy will be converted into heat, whilst a small part will create defects in the salt crystals. An important effect is the decomposition of the NaCl into (colloidal) sodium and chlorine. This process has been described by different authors: Den Hartog [1-4], Groote and Weerkamp [5], Garcia Celma [6-10]. It has been shown that energy is stored in the damaged crystals. Typical values of 10 to 1000 J/g have been estimated for the stored energy in the most heavily damaged crystals close to the waste containers [11-13]. Furthermore the amount of stored energy decays exponentially with increasing distance from the container and can be neglected at distances larger than 0.2 m. The total amount of stored energy around one HLW container is typically in the order of 1 GJ [14,15]. This energy will be released if the metallic Na and Cl_2 gas recombine to NaCl and thus restore the perfect crystal lattice. Of direct importance for the safe disposal of radioactive waste is the question whether mechanisms exist by which the stored energy can be released suddenly. If these mechanisms cannot be excluded it has to be investigated whether the release of the stored energy can create a pathway for the nuclides from the containers to the groundwater.

Stored energy can be released through the recombination of sodium and chlorine either via a thermally activated process which can be initiated if the temperature is high enough or via a spontaneous back reaction which will occur if the concentration of defects exceeds a certain percolation threshold. In differential scanning calorimetry (DSC) experiments, which are performed to measure the stored energy, the first recombination mechanism is applied. In these experiments, the temperature of the samples is gradually increased and between 200 and 300 °C [1-10,16] (depending on the heating rate) the annealing process of the radiation damage is initiated. Once this annealing mechanism starts, the released energy will cause a rise in local temperature, thus leading to a faster release of the remaining stored energy. In this way all stored energy will be released quickly. Considering the temperatures at which the radiation damage remains permanently present (< 50 °C) [11-14] there is a large safety margin for this release mechanism because an external heat source which rapidly heats the salt to 250 °C would be necessary. Such a heat source cannot in all reasonableness be imagined.

A *spontaneous back reaction* will occur if a so-called percolation barrier is exceeded. This will be the case if the concentration of decomposed salt reaches 12 to 30 volume per cent [1-4]. This implies that in cases where the sodium and chlorine segregations are *not uniformly distributed* the stored energy can be spontaneously released even if the average concentration is less than 20 to 30%. It is not clear at what (low) average local concentration the percolation barrier might be reached.
During laboratory experiments [5] some samples with an extremely high gamma energy dose were completely shattered after the DSC measurement and sometimes after the irradiation. In the fragments still a significant amount of energy was found to be stored. It is not completely clear whether this shattering of the samples is caused by a violent recombination of sodium and chlorine or by mechanical stresses due to the high pressure in the chlorine segregations.

Given the uncertainties of the model predictions and the release mechanism it has been concluded that at this moment stored energy cannot be excluded to be

released completely [1-5,12]. Therefore the thermo-mechanical consequences of a postulated release of an extremely high amount of radiation induced stored energy have been estimated [14,15]. These estimations will be reviewed in this report. The estimations are based on relations derived from a quasi-static approach, elastic material behaviour and simplified source terms. Such a quasi-static approach ignores any dynamic effects as well as fracture induced stress redistribution and therefore underestimates some of the thermo-mechanical consequences. To account for the dynamic effects and the occurrence of fractures an amplification factor has been derived from mining experience with explosives [14]. A validation of the magnification factor has been given using post experimental observation of two nuclear explosions in a salt formation.

2. MODELS FOR THERMO-MECHANICAL CONSEQUENCES

2.1 Introduction

Given the uncertainties in the release mechanism, detailed numerical analyses of the thermo-mechanical consequences have not yet been performed and analytical approximations were considered to be more appropriate [14]. These approximations are based on solutions for point and line sources in a homogeneous elastic medium. The solutions for a *point source* are used to estimate the consequences of the release of stored energy in the rock salt around *one* container. The solution for a *line source* are used to approximate the consequences of the release of stored energy in the rock salt around *all containers* in one borehole at exactly the same moment [14].

2.2 Quasi-static solutions

2.2.1 Thermo-mechanical consequences of an instantaneous point source

The temperature distribution $T(r,t)$ due to an instantaneous heat source Q [J] acting at the origin of a spherical coordinate system is known [17, 18]:

$$T(r,t) = \frac{Q}{8\rho c\left(\sqrt{\pi\kappa t}\right)^3} e^{-\psi^2} \qquad (1)$$

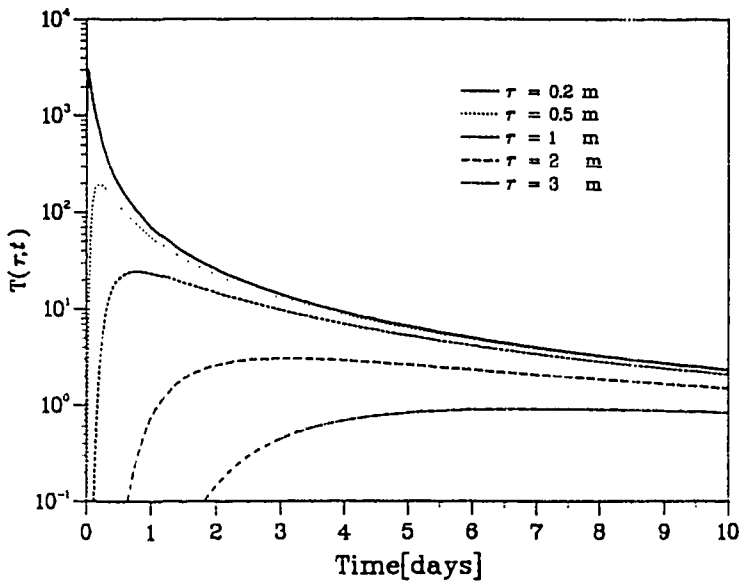

Figure 1. *Temperature distribution due to an instantaneous point source (Q = 0.66 GJ; ρ = 2160 kg/m^3; c = 920 J/(kg K); κ = 2.5 10^{-6} m^2/s).*

where:

$$\psi(r,t) = \frac{r}{2\sqrt{\kappa t}} \qquad (2)$$

κ = Heat distributivity $\lambda/\rho c$
λ = Heat conductivity coefficient
c = Specific heat
t = Time

The temperature distribution at some radial distances r from the point source is given in Figure 1. In this figure numerical values from the reference case handled in Chapter 3 are used. The temperatures in the area with $r < 0.2$ m (the container radius) have not been plotted as they are not realistic due to the point source replacing the distributed one.

The temperatures due to a distributed source can be calculated by a suitable integration of the elementary solution in eq. 1 [19].

Assuming that the acceleration effects can be neglected, the radial and tangential stresses are [17, 18]:

$$\sigma_r(r,t) = -2A\left(erf\psi - \frac{2\psi}{\sqrt{\pi}}e^{-\psi^2}\right)$$
$$\sigma_{tg}(r,t) = A\left(erf\psi - \frac{2\psi}{\sqrt{\pi}}(1+2\psi^2)\,e^{-\psi^2}\right) \qquad (3)$$

where:

$$A = \frac{E\alpha}{4\pi(1-\nu)\rho c}\frac{Q}{r^3} \qquad (4)$$

E = Youngs Modulus
α = Linear thermal expansion coefficient
υ = Poisson's ratio

Figures 2 and 3 provide graphs of the radial and tangential stresses as function of the radial distance from the origin, for several values of t. It can be observed from the figures that the radial stress is always compressive whereas the tangential stress is compressive close to the point source and tensile at larger distances. The stresses at small distances are rather high and decrease rapidly with increasing radius or time.

To obtain a more accurate picture of the spatial distribution of the radial and tangential stresses two more figures have been made with the stresses normalised with $-2A$ resp. A. Figures 4 and 5 clearly show that after a short time the radial as well as the tangential stresses approach the value $-2A$ resp A. This implies that after this initial period the stresses are proportional with r^{-3}, see eq. 4.

In order to assess these stresses, the total state of stress has to be considered. The total stress components can be found by superimposing the lithostatic pressure p on the thermal stresses. The stresses can cause fracture when fracture criteria for shear or tensile failure are met.

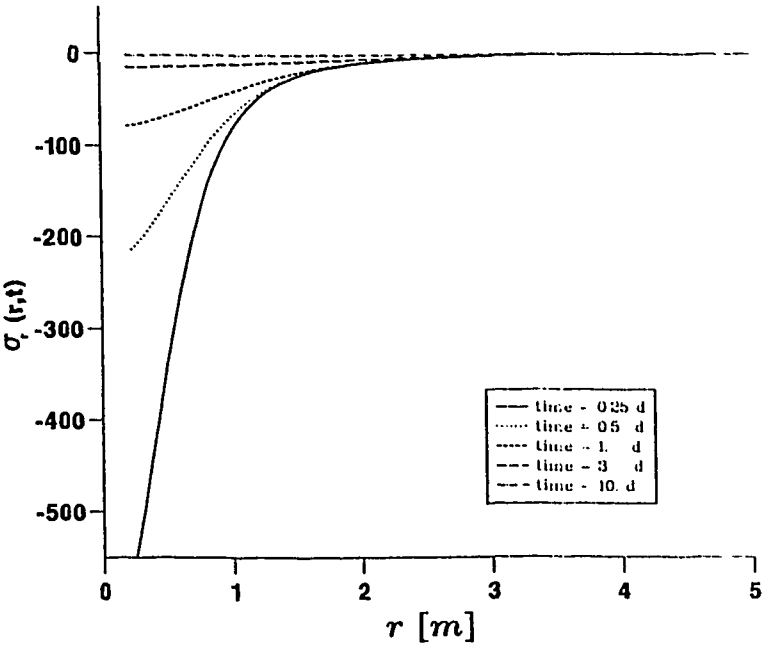

Figure 2. *Radial stress due to an instantaneous point source (Q = 0.66 GJ; ρ = 2160 kg/m^3; c = 920 J/(kg K); κ = 2.5 10^{-6} m^2/s; E = 30 GPa; υ = 0.27; α = 4 10^{-5} K^{-1}).*

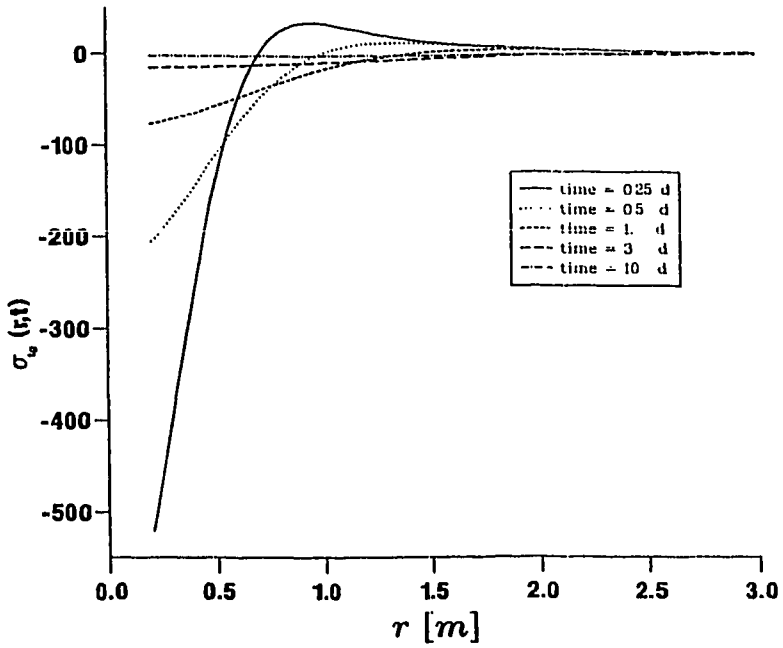

Figure 3. *Tangential stress due to an instantaneous point source (Q = 0.66 GJ; ρ = 2160 kg/m^3; c = 920 J/(kg K); κ = 2.5 10^{-6} m^2/s; E = 30 GPa; υ = 0.27; α = 4 10^{-5} K^{-1}).*

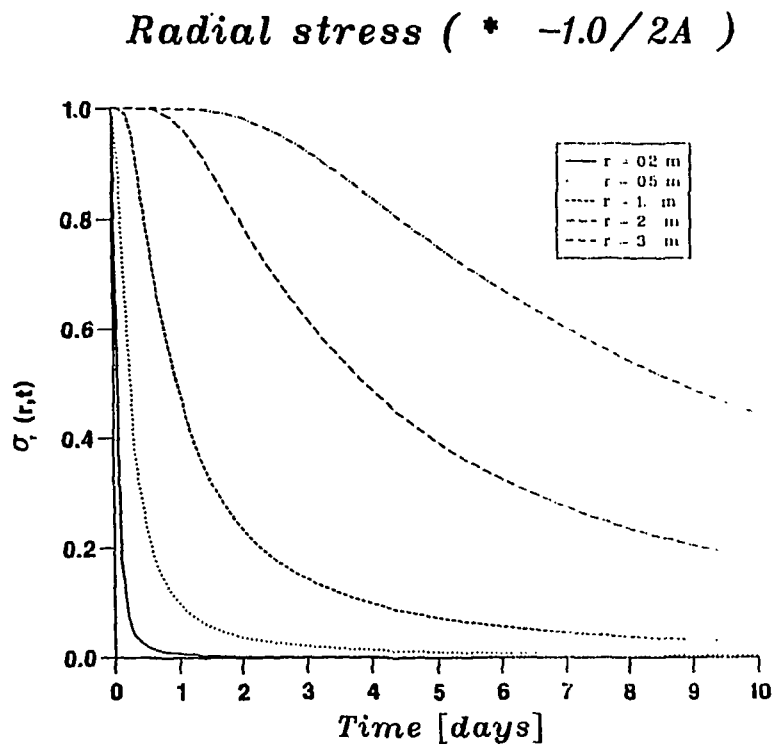

Figure 4. *Dimensionless radial stress due to an instantaneous point source.*

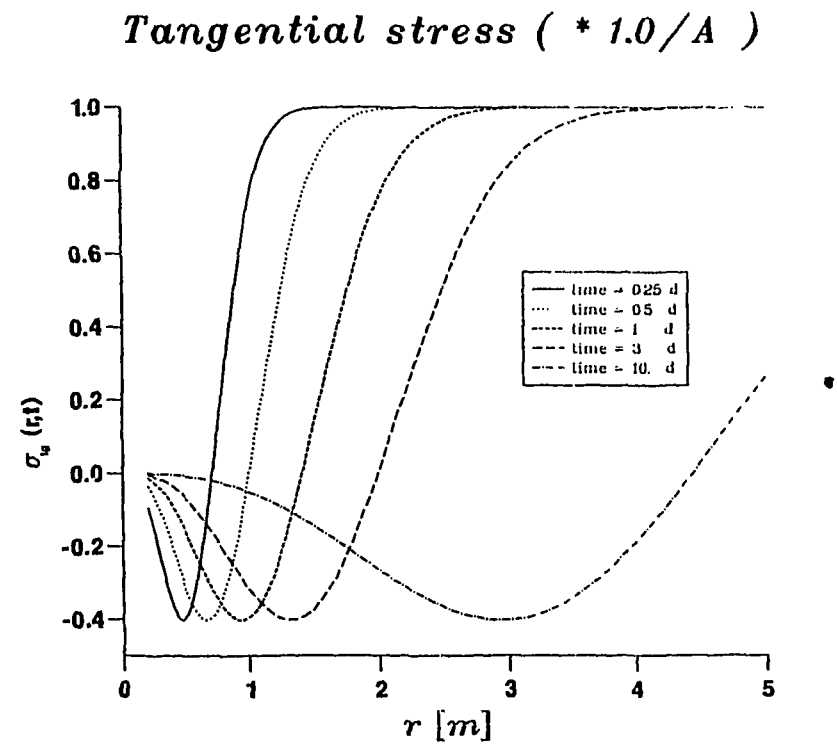

Figure 5. *Dimensionless tangential stress due to an instantaneous point source.*

Two criteria will be considered [20, 21]:

$$\text{i)}\quad \tau_{fr} = \sqrt{7T_0(\sigma_n + T_0)} \qquad \text{ii)}\quad \sigma_3 = T_0 \tag{5}$$

where:

τ_{fr} = shear strength [MPa]
σ_n = mean normal compression [MPa]
T_0 = tensile strength 2.4 MPa [20, 21]
σ_3 = maximum principal stress [MPa]

The maximum shear stress is:

$$\tau_{max} = 0.5(\sigma_{tg} - \sigma_r) = \frac{A}{2}\left(3\,erf\psi - \frac{2\psi}{\sqrt{\pi}}(3 + 2\psi^2)\,e^{-\psi^2}\right) < \frac{3A}{2} \tag{6}$$

The mean normal compression σ_n is:

$$\sigma_n = p - \frac{2\sigma_{tg} + \sigma_r}{3} = p + \frac{8A}{3\sqrt{\pi}}\psi^3 e^{-\psi^2} > p \tag{7}$$

Combining eqs. 4, 5, 6 and 7 leads to the following relation for the region where the stresses do not cause shear fracture:

$$r > r_s \equiv \left(\frac{3E\alpha Q}{8\pi(1-\nu)\rho c\sqrt{7T_0(p+T_0)}}\right)^{1/3} \Rightarrow \tau_{max} < \tau_{fr} \tag{8}$$

The tensile criterion is determined by the maximum principal stress σ_3 which equals the sum of σ_{tg} and $-p$. Realizing that the tangential stress is always less than A, the following relation for the region where the stresses do not cause tensile fracture is obtained:

$$r > r_t \equiv \left(\frac{E\alpha Q}{4\pi(1-\nu)\rho c(p+T_0)}\right)^{1/3} \Rightarrow \sigma_3 < T_0 \tag{9}$$

When fracture occurs energy will be needed to create the free surfaces. It can be anticipated, however, that this will be less than the elastic energy assumed in the analysis. This implies that the real fracture zone can be slightly larger than indicated with eqs. 8 and 9. As indicated above the neglect of dynamic effects may also lead to an underestimation of the fracture zone. The magnitude of these effects will be discussed in subchapter 2.3.

2.2.2 Thermo-mechanical consequences of an instantaneous line source

The temperature distribution due to an instantaneous line source q [J/m] acting at the axis of a cylindrical coordinate system is [17, 19]:

$$T(r,t) = \frac{q}{4\rho c \pi \kappa t} e^{-\psi^2} \tag{10}$$

The parameter ψ is given in eq. 2.

Assuming that acceleration effects can be neglected the radial and tangential stresses are [19]:

$$\begin{aligned} \sigma_r(r,t) &= -B\left(1 - e^{-\psi^2}\right) \\ \sigma_{tg}(r,t) &= B\left(1 - \left(1 + 2\psi^2\right)e^{-\psi^2}\right) \end{aligned} \tag{11}$$

where:

$$B = \frac{E\alpha}{2\pi(1-\nu)\rho c}\frac{q}{r^2} \tag{12}$$

From these equations it can be observed that the radial stress is always compressive whereas the tangential stress is compressive close to the location of the line source and tensile at larger distances. The stresses at small distances are rather high and decrease with increasing radius and time.

The assessment of these stresses has been performed in the same way and with the same criteria as with the point source. The maximum shear stress is:

$$\begin{aligned} \tau_{max} &= 0.5\left(\sigma_{tg}^2 + \sigma_r^2 - \sigma_{tg}\sigma_r\right)^{1/2} \quad \Rightarrow \\ \tau_{max} &= \frac{B}{2}\left(3 - e^{-\psi^2}(6 + 6\psi^2) + e^{-2\psi^2}(3 + 6\psi^2 + 4\psi^4)\right)^{1/2} < \frac{B\sqrt{3}}{2} \end{aligned} \tag{13}$$

The mean normal compression σ_n is:

$$\sigma_n = p - \frac{\sigma_r + \sigma_{tg}}{3} = p + \frac{2B}{3}\psi^2 e^{-\psi^2} > p \tag{14}$$

Combining eqs. 12, 13 and 14 now leads to the following relation for the region where the stresses do not cause shear fracture:

$$r > r_s \equiv \left(\frac{E\alpha q\sqrt{3}}{4\pi(1-\nu)\rho c\sqrt{7T_0(p+T_0)}}\right)^{1/2} \Rightarrow \tau_{max} < \tau_{fr} \tag{15}$$

The tensile criterion is determined by the maximum principal stress σ_3 which equals the sum of σ_{tg} and $-p$. Realizing that the tangential stress is always smaller than B, the following relation for the region where the stresses do not cause tensile fracture is obtained:

$$r > r_t \equiv \left(\frac{E\alpha q}{2\pi(1-\nu)\rho c(p+T_0)} \right)^{1/2} \Rightarrow \sigma_3 < T_0 \qquad (16)$$

When fracture occurs energy will be needed to create the free surfaces. It can be anticipated, however, that this will be less than the elastic energy assumed in the analysis. This implies that the real fracture zone can be slightly larger than indicated with eq. 16. As indicated above the neglect of dynamic effects may also lead to an underestimation of the fracture zone. The magnitude of these effects will be discussed in subchapter 2.3.

The consequences of the postulated instantaneous release have also been estimated using the relation [15]:

$$r_t = \left(\frac{E\alpha q}{\pi\rho cp} \right)^{1/2} \qquad (17)$$

This relation was derived assuming incompressible material with zero tensile strength. This relation corresponds exactly with eq. 16 for incompressible material ($\upsilon = 0.5$) without tensile strength ($T_0 = 0$).

2.3 Dynamic effects

An assumption in the solutions presented in the previous subchapter is that the dynamic effects can be neglected. The problem of the dynamic stress distribution due to an instantaneous heat source concentrated in a point has been handled by Nowacki and Parkus [17, 18]. As can be imagined the difference between the dynamic and the quasi-static solution, is noticeable only in a limited period of time. This dynamic effect also strongly depends on the time needed to release the energy and the area or volume of the source. If this time is set to zero, and the heat source is concentrated in a point, the dynamic solutions for the stresses and displacement have a discontinuity according to Nowacki [17]. Parkus, however, states that the stresses have no discontinuity in such a case [18]. To numerically investigate whether this discontinuity will occur in reality the release mechanism has to be known. As the precise release mechanism is not known it is not possible to make an accurate dynamic analysis.

There is, however, a method which can provide a reference point with respect to the importance of the dynamic effects. This method is based on the use of explosives in civil engineering and mining technology. The following procedure has been applied [14]:

i) The quasi-static solution for a point source is compared with an empirical relation for a subsurface explosion. Based on the similarity of this relation and the quasi-static solution, a dynamic amplification factor is determined and an estimate for the dynamic solution is obtained.

ii) This estimate of the dynamic solution is validated with some results of large nuclear explosions deep in salt formations.

2.3.1 Estimate of the dynamic solution based on an empirical relation

An empirical relation exists for the burial depth h needed to obtain a 'contained' explosion of yield L [22-24]:

$$h > c_1 L^{1/3} \tag{18}$$

where:

- h = the burial depth of the explosive [m]
- L = the yield of the explosive in kt (1 kt = 10^{12} cal = 4.2 TJ [22])
- c_1 = a constant which generally depends on the type of explosive and the type of rock formation. The highest factor has been found for a nuclear explosion: 110 [23] or 120 [22]. These value are based on experiments in different rocks including rock salt.

A contained yielding implies that the burial depth h is large enough to ensure that the fracture criteria are not met at the earth surface where $p = 0$. The quasi-static solutions given above then give the following prediction for the burial depth:

$$h_{Q.S} > \left(\frac{E\alpha}{4\pi(1-\nu)\rho c T_0} \right)^{1/3} Q^{1/3} \equiv c_2 Q^{1/3} \tag{19}$$

The parameter c_2 depends upon the thermo-mechanical properties. In Table 1 the relevant properties and the resulting c_2 are given for different rock types. The constitutive properties are taken from the data base set up in the OPLA phase 1 research [20], for granite the properties are from PAGIS [25]. (The results indicate that for the given rock types the use of explosives is most effective in rock salt. This is primarily caused by the high value for α and relative low value for T_0).

Table 1. *Material properties and the constant c_2 in eq. 19 for different rock types.*

Rock type	E_{dyn} [GPa]	α [$10^{-6}K^{-1}$]	υ_{dyn} [-]	ρ [kg/m^3]	c [J/(kg K]	T_0 [MPa]	c_2 [m/(kt)$^{1/3}$]
Rock salt	35.5	42.5	0.27	2160	855	2.4	54
Bischofite	20	30	0.27	1600	1350	1.0	50
Carnallite	21.5	30	0.27	1820	1200	1.5	45
Sylvite	25	37	0.27	1950	590	3.7	46
Gypsum rock	13.6	24	0.25	2300	1455	1.0	35
Anhydride	70.0	15	0.28	2900	732	5.6	35
Sandstone	40	10	0.20	2300	975	5.3	24
Shale/mudstone	44	20	0.3	2600	1240	4.5	31
Clays	0.4	30	0.49	1960	1550	0.06	35
Limestones	60	8	0.25	2050	1000	8.6	23
Chalk	18	10	0.20	1700	1500	1.3	28
Dolomite	80	7	0.35	2700	1250	10.9	20
Granite	72.8	20	0.31	2630	750	8.5	35

A comparison of the quasi-static solution with the empirical relation leads to the conclusion that the relation between the yield and the depth only differs in the factor c_1 and c_2. It can be concluded that for rock salt an amplification factor of

2.0 to 2.4 on the quasi-static solution is needed to predict the condition for contained yielding. For other rock types this dynamic amplification factor differs.
A reasonable estimate for the dynamic solution of the instantaneous point source is the product of the quasi-static solution and the dynamic amplification factor.

According to this dynamic estimate the region where the stresses do not cause shear fracture is given by:

$$r_s = 2.4\left(\frac{3E\alpha}{8\pi(1-\nu)\rho c\sqrt{7T_0(p+T_0)}}\right)^{1/3}\cdot Q^{1/3} \qquad (20)$$

And the region where the stresses do not cause tensile fracture is given by:

$$r_t = 2.4\left(\frac{E\alpha}{4\pi(1-\nu)\rho c(p+T_0)}\right)^{1/3}\cdot Q^{1/3} \qquad (21)$$

2.3.2 Validation of the dynamic estimate

The dynamic estimates can be validated with the results of two underground nuclear explosions in rock salt formations viz. the Salmon Event [26] and the Gnome shot [27].
The Salmon Event was a 5.3 ± 0.5 kt nuclear detonation at a depth of 827.8 m in the Tatum salt dome in Mississippi on October 22, 1964. The explosion created a nearly spherical and stable cavity of radius 17.6 ± 0.6 m. After the explosion two boreholes were drilled in the direct surrounding of the cavity providing samples for geophysical investigation. Radioactive melt injected into cracks was observed as far as 37 m from the shot point, and radioactivity increased above background as far as 64 m. The salt in the direct surrounding was highly microfractured and contained some macrofractures. It was found that beyond 90 to 120 m from the shot point, the rock salt approached the pre-shot condition [26].
The Gnome shot was the first Plowshare experiment. It was performed on 10 December 1961 at a depth of 360.9 m in the bedded salt formation 25 miles southeast of Carlsbad New Mexico. The fission product analyses showed that the actual yield was 3.1 ± 0.5 kt. Post explosion inspection showed that a cavity was created with a volume of nearly 1 million cubic feet, equivalent to a sphere with diameter of 38 m [27]. It was noted that the walls of the cavity and the vent path had a blue colour which is attributed to the radiation damage of the salt crystals [26]. Radial fractures about the cavity extended up to 60 m. Some of these fractures had melt injected into them 12 m from the walls [26]. Table 2 gives a summary of some characteristics of the two nuclear underground explosions.

Table 2. *Comparison of dynamic estimates with experimental values*

Experiment	depth [m]	yield [kt = 4.2 TJ]	crack length [m]	
			observed	predicted with eqs. 20 & 21
Salmon event	828	5.3 ± 0.5	90 - 120	100 - 120
Gnome shot	361	3.1 ± 0.5	60	80 - 100

The table also gives the prediction of the crack length based on the dynamic estimates given in eqs. 20 and 21. Predictions and observations for the Salmon event agree very well. The observed crack length after the Gnome shot is shorter than predicted. This is assumed to be explained by the fact that the seal of the adit was not functioning as it should be. It nevertheless can be stated that the dynamic effects and the occurrence of fracture are bound by the dynamic estimations.

2.3.3 Discussion on the dynamic estimate

The estimation of the dynamic solution is based on an amplification factor on the quasi-static solution derived from the near surface explosion experience in civil and mining engineering. Amplification factors are often used in the analyses of dynamic and shock problems [27].

A validation for the use at larger depth has been performed with two large nuclear explosions in salt formations. This validation is not a guarantee that the predictions of the crack length with the dynamic estimate are very accurate. There are quite some differences between the nuclear explosions used for the validation, the subsurface contained explosions, and the sudden release of the radiation induced stored energy in rock salt.
Some important differences between a nuclear explosion and a sudden release of energy are:

i) The amount of energy to be released is about four orders of magnitude larger in the case of the nuclear explosions.

ii) The volume in which the energy is released is different. It is stated that the nuclear bomb was no bigger than a beach ball [27] which implies a volume of about 0.5 m^3. The volume of the nuclear material is smaller, it is estimated to be 0.2 dm^3. The volume in which the radiation induced energy is released appears to be about 0.42 m^3, see below.

iii) In case of the nuclear device the amount of energy is released in a small volume installed in a backfilled cavity in the salt whereas the radiation induced energy is released directly in the salt which encloses the waste containers.

iv) The nuclear explosion being a nuclear reaction will use less time than the release of radiation induced energy being a chemical process.

ad i) and ii).
As the amount of energy and the energy density is much larger in the case of a nuclear explosion local temperatures will certainly be much higher and possible other processes will take place.

ad iii).
It is not exactly known how the nuclear device is installed in the cavity. According to [27] the cavity was originally about 15 feet in diameter which implies a volume of less than 50 m^3. The space between the device and the cavity wall has been backfilled. It can be assumed that this backfilling has been done with care because the goal of the nuclear explosions was to create as much damage to the rock as possible. Nevertheless one has to consider that some porosity will be left. This pore volume will be a portion of the initial volume of

the cavity. This means a pore volume less than 50 m^3. The thermal expansion of the material due to the release of 5 kt equals about 1200 m^3. So the pore volume is at the highest some per cents of the thermal expansion volume. In the case of the radiation induced energy the release occurs in rock salt in which the pore volume is almost zero due to the thermally induced compression in the first years after emplacement of the waste. More pore space will be left in the waste containers, in the space above and below the glass and perhaps in the cracks in the glass. Initially the empty volume above the glass is about 0.03 m^3. This pore volume will be reduced to a small fraction. The thermal expansion due to the release of 1 GJ equals about 0.06 m^3. This implies that the pore volume will be a fraction of the thermal expansion volume. This fraction is of the same order of magnitude as in the case of the nuclear explosion.

It therefore might be concluded that the possible damping effect of the pore volume will not differ substantially in both cases.

ad iv).
The effect of these differences is difficult to quantify. There, however, is no doubt that the dynamic effects due to the nuclear explosion are more severe than due to the slower chemical process.

2.4 Conclusions

It has been concluded that it cannot be excluded a priori that radiation induced stored energy will be released completely in a relatively short time. In this chapter a model has been described to predict the thermo-mechanical consequences of an instantaneous release of an extremely high amount of stored energy.

First *quasi-static models* have been used to estimate the thermo-mechanical consequences of the instantaneous release of stored energy for two idealised situations. The first is a point source which models the release of energy in the salt around one single HLW container. The second deals with a line source which models the rather unlikely case of the release of energy in the salt around all HLW containers in one borehole.
From the quasi-static model predictions it is concluded that fracture cannot be excluded in a relatively thin shell of salt directly surrounding the containers. The thickness of this fractured zone is less than 2 m.

To account for the *dynamic effects and the occurrence of fracture* a 'dynamic amplification factor' has been derived from an existing empirical relation for the effects of explosions emanating from mining engineering. The empirical relation predicts the thickness of the fractured zone to be a factor 2.4 higher than that estimated with the quasi-static method. The use of this *dynamic amplification factor* has been validated with experimental data of two nuclear explosions in salt formations. The observed crack length appears to be shorter or equal to the predicted length. The predictions were based on the quasi-static model and the dynamic amplification factor. A discussion has been given of the differences between the the nuclear explosions and the release of irradiation induced stored energy. As most factors listed make the dynamic effect of the release of radiation induced stored energy smaller it can be concluded that the dynamic amplification factor will be smaller than 2.4. It, however, will be difficult to give a more accurate prediction of the dynamic effect.

It has been concluded that the dynamic effects can be approximated with the quasi-static models and the dynamic amplification factors.

3. NUMERICAL RESULTS

3.1 Introduction

The thermo-mechanical consequences of the release of radiation induced stored energy will be quantified for the concepts studied in the framework of the national program OPLA in the Netherlands [14,15]. Some characteristic parameters of these disposal concepts are given in Tables A1 and A2. For the quantification the dynamic estimate given in the previous chapter wll be used. Furthermore the sensitivity of the different parameters will be discussed.

3.2 Numerical results for the OPLA cases

3.2.1 Amount of stored energy

The amount of energy to be released is related to the total stored energy around one container Q_t given by the relation:

$$Q_t = \int_V \gamma \rho s(x,y,z) dV = \gamma \rho \beta s_{max} V \qquad (22)$$

where:

γ	=	released energy per mole per cent decomposed salt [J/kg per mole %]
ρ	=	density [kg/m^3]
s	=	molar fraction of decomposed salt[mole %]
s_{max}	=	maximum molar fraction of decomposed salt [mole %]
ß	=	shape factor $0 < ß < 1$
V	=	volume of decomposed salt [m^3].

According to an analysis with the modified Jain-Lidiard model the region of decomposed salt has a thickness δ of 0.16 m [12]. Taking into account the container diameter d of 0.42 m, the height h of the glass equal 1.1 m, and taking into account that at the top and the bottom of the container also salt with a thickness δ of 0.16 m will be damaged the total volume V of damaged salt is:

$$V = h\frac{\pi}{4}\left((d+2\delta)^2 - d^2\right) + \delta\frac{\pi}{8}\left((d+2\delta)^2 + d^2\right) = 0.42\ \mathrm{m}^3 \qquad (23)$$

From the analysis it can be concluded that ß can be approximated with 0.5 [12, 15], see also Figure 6 [13]. Taking further a released energy γ = 70000 J/kg per mole per cent decomposed salt and a maximum molar fraction s_{max} = 20 % the magnitude of Q_t appears to be 0.66 GJ. This value corresponds with 1.6 10^{-4} kt.

3.2.2 Thermo-mechanical consequences

According to the **quasi-static approach** the extent of the fractured area can be calculated with the eqs. 8 and 9 for a point source of strength Q and the eqs. 15 and 16 for a line source of strength q.

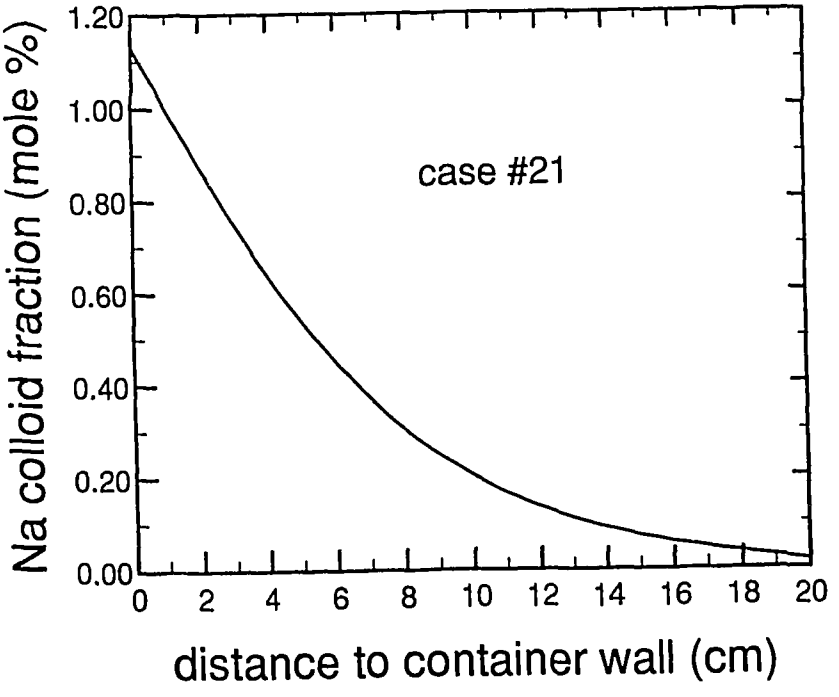

Figure 6. *Maximum colloid fraction as a function of the distance to the waste container ([13], see Table A1 and A2).*

For a *point source* these relations can be written as:

$$r_s = \alpha_s Q^{1/3} \quad \text{and} \quad r_t = \alpha_t Q^{1/3} \quad [\text{m}] \tag{24}$$

where Q is given in GJ.
For a *line source* the relations can be written as:

$$r_s = \alpha_s \sqrt{q} \quad \text{and} \quad r_t = \alpha_t \sqrt{q} \quad [\text{m}] \tag{25}$$

where q is given in GJ/m.

The constants α_s and α_t depend on the material properties and the burial depth. In Table 3 some values for these constants and resulting crack lengths are given based on the properties: $\rho = 2160$ kg/m^3; $c = 920$ J/(kg K); $E = 30$ GPa; $\upsilon = 0.27$; $\alpha = 4\ 10^{-5}$ K^{-1}.

Table 3. *Constants α and extent of fractured zone according to the quasi-static solution (Reference Case).*

depth [m]	point source (eq. 24)				line source (eq. 25)			
	α_s	r_s [m]	α_t	r_t [m]	α_s	r_s [m]	α_t	r_t [m]
700	1.8	1.6	1.6	1.4	2.6	1.0	2.7	1.6
1000	1.7	1.5	1.4	1.2	2.4	1.4	2.3	1.4
1300	1.6	1.4	1.3	1.1	2.2	1.3	2.1	1.2

The source term Q is generally less than but maximally equal to Q_t (0.66 GJ). In the analysis it is assumed that $Q = Q_t$. The source term for the line source q is generally less than but maximally equal to Q_t/ℓ. Here ℓ is the sum of the lengths of a container and a salt plug [15, 29]; $\ell = 2$ m.

This quasi-static approach shows that the unfavourable thermo-mechanical consequences of the release of all stored energy are restricted to a shell of rock salt around the waste containers. The thickness of this shell is less than 2 metres. In this shell high temperatures can occur locally during a short time period (less than 1 day). In this region the average temperature rise is < 12 °C [14,15], outside this region the temperatures of the rock salt are not increased substantially (< 5°C, see also Figure 3). The stresses in the rock salt outside the shell will change but not in such a way that cracks will initiate.

It has been shown that the **dynamic effects** can reasonably be estimated with an amplification factor of 2.4 for the point source, eqs. 20 and 21. For the line source this factor could not be estimated but it is assumed that the dynamic amplification factor is the same as in the case of a point source. The resulting estimate of the maximum extent of the fractured area is given in Table 4. For this estimate the material properties and source term are taken the same as in the previous subparagraph. It can be observed that the radial dimension of the fractured zone is the same for both the point and line source. In the unlikely case of the line source the axial extent is the same as the length of the bore hole.

Table 4. *Extent of fractured zone according to the dynamic approach (Reference case).*

depth [m]	for a point source [m]	for a line source [m]
700	3.2 - 3.7	3.6 - 3.8
1000	2.9 - 3.6	3.2 - 3.3
1300	2.7 - 3.4	2.9 - 3.1

3.3 Discussion of the numerical results.

3.3.1 Amount of stored energy Q_t

The amount of stored energy has been determined with eq. 22. This equation can be considered to be correct but the factors have some uncertainties which will be discussed.

$$Q_t = \gamma \rho \beta s_{max} V \qquad (26)$$

3.3.1.1 The released energy decomposed salt γ

γ is taken to be 70 J/g per mole per cent coloidal Na. This value is based on 4.25 eV per F-H pair [5, 11]. Recent measurements [5], however, have shown that 8 eV per F-H pair is a better value. This means that the value for γ of 125

J/g per mole per cent colloidal Na has to be taken into account. There also are measurements on Spanish salt where values as high as 159 J/g per mole percent colloidal Na have been found (de Las Cuevas in [10]).

3.3.1.2 The density ρ

ρ can be considered to be rather accurate. A recorded range from 2100 to 2200 kg/m^3 is reported [20].

3.3.1.3 The maximum molar fraction of decomposed salt s_{max}

s_{max} is calculated with a Jain-Lidiard model and happens to be 4 % for the typical disposal concept: mine and waste strategy C [12,14,15]. In the consequence analysis s_{max} is taken to be 20 %. This value is based on the percolation theory [30] where values are given for different types of crystal lattice structures. For a simple cubic lattice the value is 25 % and for a faced centred cubic (fcc) lattice 12 %. It must be realised that the radiation damage is built up in the Cl sublattice which is a fcc lattice. So a value of 12 % would have been a better estimate of s_{max}.

3.3.1.4 The shape factor ß

ß is taken to be 0.5. This factor implicitly is defined as:

$$\beta = \frac{1}{V}\int_V \frac{s}{s_{max}}\,dV \equiv \frac{1}{V}\int_{r_o}^{\infty} f(r)2\pi r\,dr \qquad (27)$$

The shape factor ß can be derived from $f(r)$, the spatial distribution of s. Results of Jain-Lidiard analyses in which the proper relations between s and the time dependent temperature, dose and dose-rate have been incorporated can be used to derive the spatial distribution of s. Figure 6 shows a typical calculated radial distribution of the maximum colloid fraction. It can be observed that the decrease of s is stronger than linear and even stronger than an exponential decay. If one assumes that s is a linear function of the distance, then eq. 27 leads to ß = 0.47. If one assumes that s has an exponential decay:

$$\frac{s(r)}{s_{max}} = f(r) = e^{-c(r-r_o)} \qquad (28)$$

the constant c can be derived from the results in Figure 6. It then appears that c = 14.7 [m^{-1}] which is based on a reduction of a factor 1.8 in the first 4 cm. It can be noted that this reduction in the amount of stored energy is the same as the reduction of the calculated deposited energy [12]. This implies that in this region there is a linear relation between the stored energy and the deposited energy. Using this value of c eq. 27 gives ß equal to 0.37.

3.3.1.5 The volume of decomposed salt V

V is calculated assuming that in the salt further away than 16 cm (δ) from the container there is no colloid formation. As can be seen in Figure 6 this is reasonable. It must be recognized, however, that the colloid fraction is not exactly zero at the distance of 16 cm. Based on the exponential decay used above 91% of the energy is stored in the region with a radial 'thickness' less than 16 cm.

3.3.2 Amount of released energy Q

In the previous analysis of the thermo-mechanical consequences it has been assumed that all stored energy will **suddenly** be released. This is a conservative assumption since experiments show that during such sudden back reactions, only a fraction of the total stored energy is released [5].

3.3.3 Geometrical approximation of the source

The real geometry of the heat source is rather complicated. It is determined by the region of the damaged salt and therefore consists of a 'chain line' of thick-walled cylindrical shells with thick end caps. The thickness of the shell of fractured rock salt around one HLW container is assumed not to deviate substantially from the fractured zone in the case of a point source.
The reasons for this assumption are the small differences between the fractured zone in the point and line source and the fact that the fractured zone is large in comparison with the dimension of the source.

3.3.4 Summary

Table 5 summarizes the different values of stored energies and extend of fractured zones from which the influence of the different parameter values can easily be derived. It has been assumed that all stored energy is released and the relations for the depth of 700 m are taken from Table 3.

Table 5. *Summary of results of the instantaneous release of stored energy related to one HLW container.*

Case	Parameter values				Q_t [GJ]	extend of fractured zone [m]	
	γ [J/g%]	s_{max} [%]	ß [-]	δ [m]		quasi-static	dynamic estimate
Reference	70	20	0.5	0.16	0.66	1.6	3.8
Variant 1	125	25	0.5	0.16	1.4	2.0	4.8
Variant 2	125	12	0.37	n.a.	0.55	1.5	3.5
Variant 3	70	4	0.37	n.a.	0.10	0.8	2.0

The *reference case* is used in the consequence analysis presented above.

Variant 1 takes into account the higher value for the energy per defect pair γ and the higher value for the percolation limit s_{max}. Consequently the resulting Q_t can be considered as an upper bound for the maximum amount of stored energy.

Variant 2 assumes an exponential decay of the stored energy and does not account for a 'cut-off' of the stored energy. The value for Q_t in this case can be considered as the best estimate of the maximum amount of stored energy.

Variant 3 is based on Jain-Lidiard analyses and gives at this moment the best estimate of the amount of stored energy. It can be anticipated that a lower amount of stored energy will be predicted if effects of the fractal dimension of the coloids are taken into account [31]. The presence of impurities, however, may increase the predicted amount of stored energy.

3.4 Conclusion

It can be concluded that the best estimate of the extent of the damaged zone due to the postulated instantaneous release of the stored energy is less than 5 m. Any cracks that might conceivably occur will thus remain restricted to a minor area, compared with the 100 to 300 m thick shield of salt around the repository. Moreover these cracks would heal due to creep and recrystallisation [32] in a relatively short time, less than 10 years.

4. SAFETY CONSEQUENCES

This report deals with the possible safety consequences of radiation induced stored energy in rock salt. The starting point of the report is the wide range in the model predictions of the amount of stored energy: 10 to 1000 J/g in the most heavily damaged rock salt close to the HLW containers. This wide range is caused by differences in the disposal concepts but also by uncertainces in the models. If the release of the stored energy is a slow process the consequences are fully covered by the normal design calculation of the temperatures and stresses where it has been assumed that all radiation energy is converted into heat. These analyses, however, do not cover the consequences if the release of energy is so quick that dynamic effects should be accounted for. The existence of such violent release mechanisms is doubtfull if the amount of stored energy is as low as the best estimate value of 10 to 100 J/g. For the higher values which are in the range of 1000 J/g, however, such a mechanism cannot be excluded. An upper limit analysis of the consequences of radiation induced stored energy therefore has to be based on the assumption that all stored energy will be released instantaneously which means in an explosive way.

The consequence analysis of this assumed explosive release is based on relations derived from a quasi-static approach, elastic material behaviour and simplified source terms. Such a quasi-static approach ignores any dynamic effects as well as fracture induced stress redistribution and therefore underestimates some of the thermo-mechanical consequences. To account for the dynamic effects and the occurrence of fractures an amplification factor has been derived from mining experience with explosives. This factor is 2.4 on the extent of the fractured area. A validation of the amplification factor has been given using post experimental observations of two nuclear explosions in a salt formation.

For repository conditions from the design concepts studied in the Netherlands the radial extent of the fractured area around a HLW container appears to be smaller than 5 m. This is a small value compared with the distance between individual boreholes and a very small value compared with the distance between the boreholes and the boundary of the salt formation which is more than 100 m. It is therefore concluded that it is very unlikely that the release of radiation induced stored energy leads to a pathway for nuclides from the waste containers to the groundwater around the salt formation.

The consequences of such an unlikely pathway are nonetheless covered in the performance assessment of a repository in rock salt. This has been done via the umbrella scenario 'groundwater intrusion/extrusion' or 'flooding scenario'[33, 34-36]. In these scenarios it is assumed that groundwater *intrudes* into the repository, comes into contact with the radioactive waste, corrodes the steel containers and leaches out the nuclides from the glass. Driven by the convergence of the backfilled openings which are part of the repository the contaminated brine will be *extruded* from the repository. The groundwater contaminated in this way will reach the biosphere. These scenarios are considered to cover the consequences of a by-passing of the isolation shield. The consequences are calculated independent of the mechanism leading to the groundwater intrusion. The maximum individual exposure is lower than 10^{-8}Sv/a and occurs more than half a million years after disposal [36]. This value is calculated for groundwater intrusion directly after closure of the repository. The consequences are sensitive for the moment of groundwater intrusion [15, 33, 36]. If the intrusion starts some time after closure the creep induced convergence of

the openings has reduced the volume of the pores in the backfill which implies a lower volume of intruded groundwater and consequently a lower volume of extruded contaminated brine.

In the unlikely case that the groundwater intrudes through the pathway created by the explosive release of radiation induced stored energy this will occur more than 100 years after disposal when the maximum amount of stored energy is reached [13,37]. This implies that the given value of 10^{-8}Sv/a is an upper bound for the radiological consequences.

5. SUMMARY AND CONCLUSIONS

There are a number of uncertainties in the models used in the analysis of the amount of stored energy and the consequences of a possible release. There are also processes not explicitly handled which could aggravate or mitigate the consequences. An example of an aggravating process is a possibly violent reaction between the glass and the molten salt in case of a sudden release of a large amount of stored energy. A processes which could mitigate the consequences is an intermeditate recrystalisation of the damaged crystals.

In this report the consequences have been estimated with models using conservative to best estimate parameter values. The conclusions of these estimations can be summarized:

i) It is assumed that an explosive release of the radiation induced stored energy in a repository cannot be excluded. It should be noted however, that model predictions for repository conditions indicate a small amount of stored energy, which will be released in a very smooth way.
ii) It is unlikely that an explosive release mechanism leads to a pathway for nuclides from the waste containers to the groundwater. There is a safety margin of one to two orders of magnitude.
iii) The radiological consequences of groundwater intruding into the repository through such an unlikely pathway are very low, $< 10^{-8}$ Sv/a.

These conclusions underline the large margins of safety in the contemporary repository designs with respect to the consequences of radiation induced stored energy. The consequences can be mitigated further with changes in the design. By using extra shielding containers the amount of stored energy can be decreased by one or more orders of magnitude. If the containers have a wall-thickness of at least 20 cm the built up of damage can completely be inhibited [37].

6. REFERENCES

[1] H.W. den Hartog, "Stralingsschade in NaCl, Verslag deelonderzoek REO3 over de periode 1 maart 1987 tot 1 sept. 1987," Groningen (1987),

[2] H.W. den Hartog. "Stralingsschade in NaCl, Eindrapport REO-3 over fase I van het OPLA onderzoek," Groningen (1988),

[3] H.W. den Hartog, J.C. Groote, J.R.W. Weerkamp en J. Seinen, "Eindrapportage van het onderzoek 'Stralingsschade in NaCl'," Groningen (1990),

[4] H.W. den Hartog, J. Seinen, H. Datema, J. Jacobs en H. Pol, "Radiation damage in NaCl," Groningen (1992).

[5] Jacob Groote, Hans Robert Weerkamp. "Radiation damage in NaCl: small particles," Thesis, Rijksuniversiteit Groningen (1990).

[6] A. Garcia Celma, J.L. Urai and C.J. Spiers, " A laboratory investigation into the interaction of recrystallisation and radiation damage effects in poly-crystalline salt rocks,". CEC report EUR-11849-EN (1988),

[7] A. Garcia Celma, H. van Wees and L. Miralles, "Sample preparation for the HAW project and experimental results from the HFR," ECN report ECN-C--90-014 (1990),

[8] A. Garcia Celma, "Sample preparation for the HAW and HFR irradiation experiments," ECN report ECN-C--91-008 (1991),

[9] A. Garcia Celma, "Stored energy in irradiated salt samples," ECN report ECN-C--92-055 (1992),

[10] A. Garcia Celma, C. de las Cuevas, P. Teixidor, L. Miralles and H. Donker, "On the possible continuous operation of an intergranular process of radiation damage anneal in rock salt repositories," paper presented at the Int. Symp. on Geological Diposal of Spent Fuel, High Level and Alpha-bearing wastes, Antwerp, Belgium, 19-23 October 1992.

[11] J. Bergsma, R.B. Helmholdt and R.J. Heijboer, *Nuc. Techn.* **71** (1985) 597.

[12] J.B.M. de Haas en R.B. Helmholdt, "Stralingsschade rond KSA-containers in steenzout," ECN report ECN-89-23 (1989).

[13] W.J. Soppe and J. Prij, *Nuc. Techn.* (1994), in press.

[14] J. Prij, "On the design of a radioactive waste repository," Thesis University Twente (1991).

[15] J. Prij et al, " Safety evaluation of disposal concepts in rock salt (VEOS). Final report, part 1: Summary and Evaluation," ECN/RIVM, jan. 1989.

[16] G. van Opbrock, H.W de Hartog, *J. Phys. C* **18** (1985) 257. (1985).

[17] W. Nowacki, "Thermoelasticity," Pergamon Press, (1962).

[18] Heinz Parkus, "Instationäre Wärmespannungen," Wien Springer Verlag, (1959).

[19] R.J. Wart et al, "Benchmark Problems for Repository Design Models," NUREG/CR-3636, (1984).

[20] J. Prij et al, "De invloed van inhomogeniteiten op de isolatiecapaciteit van een zoutvoorkomen," Eindrapport REO-4, ECN-87-113 ECN/RGD/RUU (1987).

[21] J. Prij et al, "Safety evaluation of disposal concepts in rock salt (VEOS). Final report, part 5: Spannings- en vervormingsberekeningen," ECN/RIVM, april 1988.

[22] Autoren kollektiv, " Handbuch Sprengtechnik," VEB Deutscher Verlag für Grundstoffindustrie, Leipzig, (1975).

[23] K. Parker, "Nuclear Explosives: A Tool for the Mining Engineer?" *The Mining Engineer*, **123**, 133, December 1970.

[24] H.W. Wild, "Sprengtechnik in der Bergbau, Tunnel- und Stollenbau sowie in Tagebau und Steinbrüchen," Verlag Glückauf GmbH, Essen, (1984).

[25] F. Van Kote et al, "Enfouissement dans des formations granitiques, Project PAGIS," EUR 11777 FR. Commission des Communautés eu1988.

[26] D. Rawson et al, "Post-Explosion Environment Resulting from the Salmon Event," *Journal of Geophysical Research,* **71**, No. 14, 3507, (1966).

[27] Nuclear News-ANS-January 1963-19, "Nuclear Explosives-coming soon".

[28] Ray W. Clough, "Dynamics of structures," Mc. Graw Hill Inc. 1975.

[29] Van Hattum and Blankevoort, "Locatie-onafhankelijke studie inzake de aanleg, bedrijfsvoering ....." (1986).

[30] Dietrich Stauffer, "Introduction in percolation theory," Taylor and Francis, Londen 1985.

[31] W. J. Soppe, *Nucl. Instr. Meth. Phys.* **B65** (1992) 493.

[32] N.C. Brodsky, "Crack Closure and Healing Studies in WIPP Salt Using Compressional Wave Velocity....," SAND90-7076, November 1990.

[33] R. Storck et al, "Performance Assessment of Geological Isolation Systems .....(PAGIS). Disposal in Salt Formations," EUR 11778 EN (1988).

[34] J. Prij et al, "Safety evaluation of geological disposal concepts for low and medium-level wastes....(Pacoma project)," EUR 13178 EN (1991).

[35] R.P Hirsekorn et al, "Performance Assessment of Confinements for .....(PACOMA). Rock Salt Option," GSF-Bericht 12/91 (1991)

[36] J. Prij et al, "PRObabilistic Safety Assessment (PROSA) Final report," ECN/RIVM/RGD (1993).

[37] W.J. Soppe, H. Donker, A. Garcia Celma, J. Prij, "Radiation induced stored energy in rock salt, A review", *J. Nucl. Mat.* (1994), in press.

NOMENCLATURE

A	Normalized stress for the point source, eq. 4
B	Waste strategy
B	Normalized stress for the line source, eq. 12
C	Waste strategy
c	Specific heat
d	Diameter of the waste container
E	Young's modulus
h	Burial depth, eq. 18
L	Yield of an explosive, eq. 18
p	Rock pressure
Q	Amount of stored or released heat
q	Amount of released heat per unit of length
r	Radial coordinate
s	Molar fraction of decomposed NaCl.
T	Temperature (rise)
T_0	Tensile strength of rock salt
t	Time
V	Volume
x	Cartesian coordinate
y	Cartesian coordinate
z	Cartesian coordinate

Greek symbols

α	Coeficient of thermal expansion
ß	Parameter in yield versus burial depth relation, eq. 19
ρ	Density
δ	Thickness of the region with radiation damage
γ	Released energy per mole per cent decomposed NaCl
λ	Heat conductivity coefficient
κ	Heat distributivity $\lambda/\rho c$
υ	Poisson's ratio
η	Energy storage efficiency
σ	Normal stress
τ	Shear stress

Subscripts

eq	equivalent
fr	fracture
i,j	Indices referring to the Carthesian coordinates
n	Normal
r	Radial
s	Shear
t	Tension
tg	Tangential

TABLES

Table A1. *Characteristic parameters of the disposal concepts studied [13]*

Case No.	Formation Type	Disposal Technique	Cooling Time [a]	Interim Storage [a]	Disposal Depth [m]	Geothermal Temp. [°C]
11	pillow	borehole	3	50	616	29.4
12	pillow	borehole	10	50	616	29.4
15	pillow	borehole	3	10	619	29.5
16	pillow	borehole	10	10	619	29.5
17	pillow	mine	3	50	654	30.2
21	pillow	mine	3	10	654	30.2
22	pillow	mine	10	10	654	30.2
23	dome	borehole	10	10	957	36.6
24	dome	mine	10	10	1048	38.5

Table A2. *Calculated data for the salt at zero distance from the HLW container [13]*

Case No.	T_{max} [°C]	t_{max} [a]	T_{500} [°C]	K_i [krad/hr]	K_{10} [krad/hr]	D [Grad]	c_A^0 [%]	c_A^{max} [%]	t_{ca}^{max} [y]	c_{s0}^{max} [ppm]
11	65	5.3	32	3.7	2.9	1.73	0.07	0.07	$1{\cdot}10^4$	$1{\cdot}10^4$
12	64	6.2	34	3.1	2.4	1.56	0.07	0.07	$2{\cdot}10^4$	$1{\cdot}10^4$
15	118	4.4	35	11.6	8.1	4.02	0.25	0.25	$1{\cdot}10^4$	100
16	109	4.4	39	8.8	6.5	3.44	0.26	0.26	370	5000
17	70	12.3	34	25.3	19.6	11.97	0.60	0.95	$1{\cdot}10^5$	$1{\cdot}10^4$
21	129	12.3	36	75.0	52.5	27.30	1.15	1.26	$2{\cdot}10^5$	100
22	118	12.3	40	58.5	43.7	23.59	1.42	1.60	$2.6{\cdot}10^5$	200
23	116	4.4	47	8.8	6.5	3.44	0.26	0.26	370	100
24	113	9.8	47	58.5	43.7	23.59	1.70	2.23	$1.8{\cdot}10^5$	1000

T_{max} = maximum temperature
t_{max} = time at which the maximum temperature is reached
T_{500} = temperature after 500 years
K_i = initial dose rate
D = total dose

c_A^0 = maximum colloid fraction for pure NaCl
c_A^{max} = maximum colloid fraction for impure NaCl
t_{ca}^{max} = time at which c_A^{max} is reached
c_{s0}^{max} = impurity concentration for which c_A^{max} is obtained